Synthesis and fluorescence emission properties of D-*π*-D monomers based on dithieno[3,2-*b*:2',3'-*d*]thiophene

Chuan-Zeng Wang,[a] Jung-Hee Do,[a] Xing Feng,*[b] Taisuke Matsumoto,[c] Junji Tanaka,[c] Carl Redshaw,[d] and Takehiko Yamato*[a]

We herein present four highly fluorescent and stable D-π-D monomers (**2**), which were designed and synthesized using different types of aryl substituent as the donor via a Suzuki-Miyaura coupling reaction. We have studied these four symmetrical chromophores by UV-vis absorption and fluorescence emission spectroscopy both in solution and the solid state. This research shows that the introduction of the aryl groups can effectively extend the conjugation length of thiophene chromophore resulting in a shift of the wavelength of the absorption and fluorescence emission and an improvement of the fluorescence quantum yields. The notable optical features of their solid-state powders also exhibited a distinct red-shift in comparison with the emissions of their dilute solutions. These results combined with the theoretical calculations (B3LYP/6-31G*) indicate that these systems are promising candidates in the fabrication of organic electroluminescence devices.

Introduction

Heterocyclic compounds continue to attract interest due to their unique physicochemical properties, the latter suggesting that such compounds have great potential for the development of functional organic materials,[1] biochemical materials,[2] dyes,[3] and agrochemicals[4] *etc*. As a representative of unsaturated five-membered heterocyclic compounds, thiophene stands out as it possesses the highest aromatic behaviour with a high resonance energy (29 kcal mol^{-1}).[5] As a consequence, thiophene and oligothiophenes have emerged as attractive core units, and are receiving increasing attention. As expected, fused thiophenes can provide more competitive advantages with their more rigid planar *π*-conjugated geometry, stronger donor properties, and a decreased HOMO-LUMO gap.[6] Dithieno[3,2-*b*:2',3'-*d*]thiophene (DTT), with three annulated thiophene rings, is an important building block for a wide variety of functional organic materials. In particular, DTT has been employed in materials acting as the active layer in organic thin-film transistors (OTFTs).[7] A remarkably broad scope of function has been demonstrated by tuning the substituents of DTT, which can exhibit π-stacking interactions, high charge transport, and low-energy electronic transitions.[8] In this context, a promising strategy to access further materials, such as full colour OLED-based displays, has been established. Recently, this problem was solved by the introduction of bulky or heavily branched side chains into the DTT molecules or co-polymerization with a suitable bulky co-monomer. More recently, it was reported that thiophene derivatives can be used as blue-emitting materials in OLEDs by introducing long or branched side chains.[9]

To fully realize the potential of DTT based organic molecules as candidates for OLEDs, we present herein the first examples of the synthesis and photophysical properties of a new series of planar, π-conjugated pure-blue light-emitting molecules, namely, 2,6-bisaryl substituted DTTs derivatives. The π-functionalized arylboronic acids groups were successfully introduced at the thiophene core 2,6-positions affording a planar molecular structure by using a modified Suzuki-Miyaura coupling reaction (Scheme 1). As fruit fly in the photochemical material industry,[10] the introduction of 7-*tert*-butyl-1-pyrene substituents into the DTT molecule is expected to improve the photophysical properties due to its unique properties.[11] The introduction of the arylboronic acids groups is expected to extend the conjugation length of the thiophene chromophore resulting in a shift of the wavelength of the absorption and fluorescence emission into the pure blue visible region of the electromagnetic spectra and an improvement of the fluorescence quantum yields. The substituents on the thiophene molecules at the 2,6-positions were anticipated to inhibit the close face-to-face π-stacking interactions between DTTs units, and finally to lead to an improvement in the high solubility and high thermal stability of these molecules. In addition, the synthesis of four D-π-D chromophores **2** starting from dithieno[3,2-*b*:2',3'-*d*]thiophene is also described.[12] Furthermore, studies on the electronic UV-Vis absorption and fluorescence emission properties of these molecules is presented with the support of density functional theory (DFT) calculations.

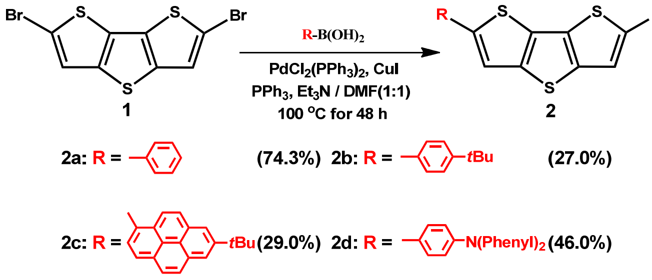

Scheme 1. Synthesis of DTT-based monomers **2**.

Results and discussion

Synthesis and characterization

The modified Suzuki-Miyaura cross-coupling reaction of the dibrominated DTT [13] with various kinds of arylboronic acids was conducted at room temperature for 24 h in dry THF. The corresponding 2,6-bisaryl substituted DTTs derivatives **2a-d** were afforded in excellent yields (recrystallization yields) as different coloured fluorescent solids (Scheme 1).

All structures for these novel thiophene derivatives **2a-d** were fully characterized based on their $^1H/^{13}C$ NMR spectra (see Figures S1-7 in the Supporting Information). Simultaneously, the structures of **2a-d** were also established on the basis of the base peak molecular ion at *m*/*z* 348.01, 460.08, 708.12, and 682.13 in their mass spectra. All results were consistent with the proposed structures. On the other hand, these four 2,6-bisaryl substituted DTTs **2a-d** are stable solids that can be stored in air at room temperature for a prolonged period of time. All these compounds have good solubility in common organic solvents including hexane with high melting points of up to 280 °C, 290 °C, 332 °C and 302 °C, respectively.

In order to investigate the target molecules in detail, suitable crystals of compound 2b were obtained as pale yellow prisms by using a binary solvent system of $CHCl_3$ (in) and hexane (out). This monomer was obtained as yellow needles and provided excellent quality data. The compound 2b crystallizes in the orthorhombic crystal system with space group $Pna2_1$. This structure is a symmetric system and the phenyl ring and DTT ring are in the same plane. The structure of 2b reveals a nearly planar molecular conformation with a packing arrangement consisting of off-set stacked dimers (Figure 1). The ditienothiophene molecules exhibit essentially an all-coplanar arrangement throughout the molecules, including the DTT units, and thus support the desired extension of the π-conjugated system. Close inspection reveals that the torsion angles are 7.64° and 3.42° between the DTT core and the terminal substituents, respectively. As shown in Figure 1b, the present molecule 2b is packed in a herring-bone pattern in a single dimension. Interestingly, an infinite molecular chain ladder-like structure (Figure 1c) was formed by intermolecular interactions with a distance of 3.234 Å (S3-C1) between neighbouring thiophene rings; meanwhile, C–H•••π (2.850 Å) interactions were observed in the supramolecular assembly. No significant π-stacking interactions between the neighbouring thiophene rings were observed, and these results strongly indicated that the two bulky *tert*-butyl groups attached to the benzene rings of the rigid DTT core play an important role in suppressing the formation of π-π stacking in the solid state.

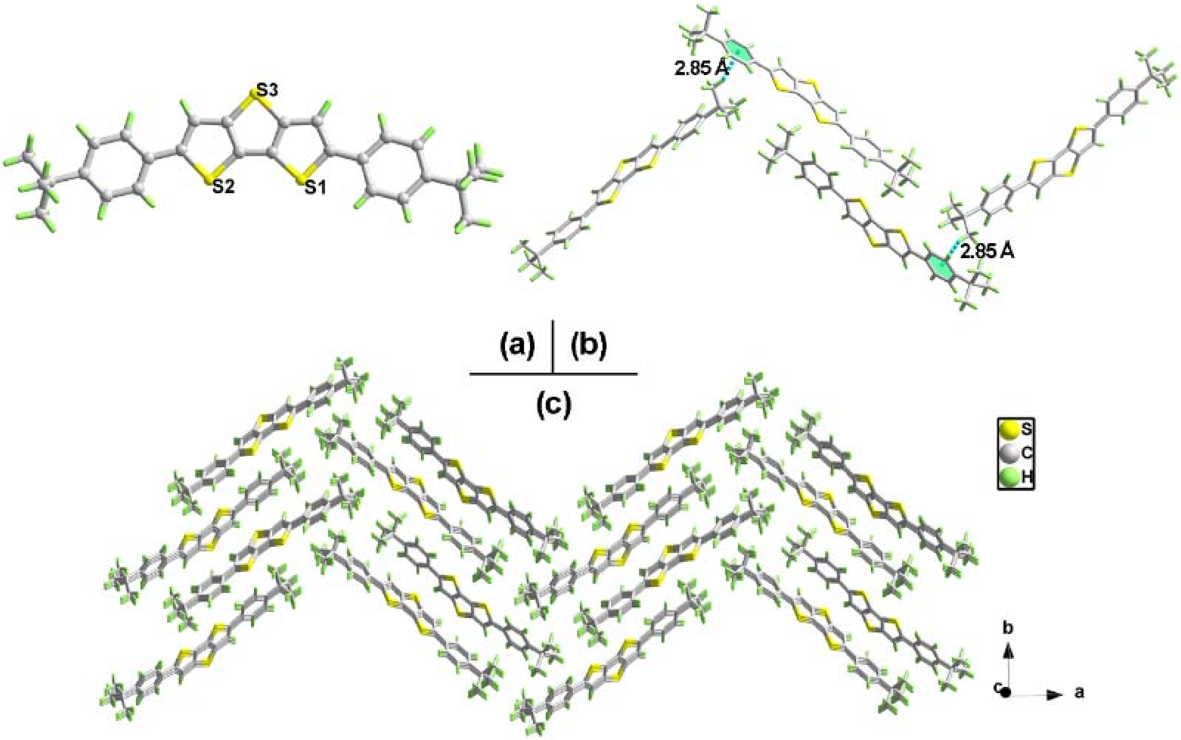

Figure 1. (a) Crystal structure of compound **2b**; (b) detailed interactions between the neighbouring DTT molecules; (c) an overall view of the stacking of the self-assembly along the *c* axis.

Photophysical properties

For the series of substituted 2,6-bisaryl substituted DTTs derivatives **2**, the electronic absorption and fluorescence-emission data were recorded and are summarized in Table 1. The UV-Vis absorption spectra of the 2,6-bisaryl substituted DTTs derivatives **2** in CH_2Cl_2 along with DTT are shown in Figure 2a. The spectra were recorded in dilute CH_2Cl_2 (~10^{-5} M) at room temperature. Compared with the value for the DTT core at 291 nm, the maximum absorption wavelength of the D-π-D monomers **2** are observed more than ca. 78 nm red-shifted to 369 (**2a**), 370 (**2b**), 399 (**2c**), and 414 (**2d**). As expected, the molecular geometries of the D-π-D structures have an impact on the optical properties primarily due to intramolecular charge transfer (ICT). It is worth noting that among these compounds **2**, the 7-*tert*-butyl-1-pyrenyl substituted DTT monomer **2c** and the *N*,*N*-diphenylamino phenyl substituted DTT monomer **2d** display the largest bathochromic shift of the absorption bands, which could be attributed to the strongest electron donating nature of pyrene and *N*,*N*-diphenylamino group compared to phenyl or 4-*tert*-phenyl groups, respectively. This result also shows a significant substitution effects in the UV-Vis spectra of **2**. On increasing the electron donating nature of the substituent, the UV-Vis spectra were found to exhibit increased bathochromic shifts in the order **2a** < **2b** < **2c** < **2d**. Also the absorption spectra in the solid state were recorded, and compounds **2a** and **2b** were found to exhibit small blue-shifts in comparison with their absorption spectra in dilute solution. It is assumed here that H-aggregate formation may occur in the solid state.[15] Further, we obtained nearly consistent absorption spectra in the solid state (film) for compounds **2c** and **2d** in comparison to the results in the dilute solution **(**see Figure S8 in the Supporting Information).

A dilute solution (~10^{-7} M) of compound **2** along with DTT in dichloromethane at room temperature on excitation at each absorption maximum exhibits a broad band blue emission (Figure 2b). Compared with the lower energy emission band of DTT, the emission band of **2a**, **2b**, **2c**, and**2d** were found to be bathochromic shifted at 411, 415, 498, and 471 nm, respectively.

Upon excitation, the fluorescence spectra of **2a**, **2b**, and **2d** exhibited a sharp peak at $\lambda_{\text{em max}}$ = 411, 415, and 414 nm with a shoulder, respectively. The emission spectra of **2c** displays a single broad peak at 498 nm. Clearly, the ITC behaviour in molecules **2** would be transformed with the introduction of donor groups at the 2,6-positions.[16] On increasing electron-donating ability of the group, a gradual bathochromic shift in the $\lambda_{\text{em max}}$ was clearly observed in the order **2a** ≈ **2b** < **2d** < **2c**. Although the origin of such transitions is uncertain, we assume that the transitions could be attributed to the aggregation or excimer formation, due to the different aryl substituents. The fluorescence quantum yields of **2a-d** and DTT recorded in dilute CH_2Cl_2 solution at room temperature are also listed in Table 1. We found the Φ_f values of **2a-c** and DTT to be in the range of 0.01–0.35. The quantum yields of the D-π-D monomers are higher than the parent compound DTT, which further indicates that ICT plays an important role in lowering the energy gap.

The fascinating properties of the monomers inspired us to investigate their luminescent performance in the solid state. Although the four DTT-based monomers displayed slight bathochromic and hypsochromic shifts in their UV-Vis absorption spectra, the compounds as films exhibited significant bathochromic phenomena in their emission spectra, and displayed $\lambda_{\text{film, max}}$ values of 491 nm, 495 nm, 525 nm, and 523 nm, respectively. Compared with their corresponding emission spectra in solution, the red-shift range is 27–80 nm (80 nm for **2a**, 80 nm for **2b**, 27 nm for **2c**, and 52 nm for **2d**, respectively). These results are probably due to the planar π-conjugated structures that tend to form dimers, which is consistent with the absorption spectra (see Figure S8 in the Supporting Information). In general, the inclusion of different types of aryl substituents with differing electron-donating ability has led to significant effects on the observed photo-physical properties, behaviour which might be interpreted in terms of donor-induced intramolecular charge transfer.[17]

Table 1. Optical absorption and emission spectroscopic data of compounds **2** and DTT.[a]

Compounds	λ_{max}abs[nm]		λ_{max}PL[nm][c]		Stokes-shift [nm]		Φ_f[d]	
	Sol.[a]	Film[b]	Sol.[a]	Film[b]	Sol.[a]	Film[b]	Sol.[a]	Film[b]
DTT	291	nd[e]	374	nd[e]	83	nd[e]	0.01	nd[e]
2a	369	363[14]	411	491	42	128	0.32	0.48
2b	370	346	415	495	45	149	0.35	0.52
2c	399	417	498	525	99	108	0.20	0.35
2d	414	419	471	523	57	104	0.34	0.50

[a] All measurements were performed under degassed conditions. [b] ~ × 10^{-5} M in CH_2Cl_2, λ_{abs} is the absorption band appearing at the longest wavelength. [c] ~ × 10^{-7} M in CH_2Cl_2, λ_{ex} is the fluorescence band appearing at the shortest wavelength. [d] Wavelength of excitation. [e] Absolute quantum yield (± 0.01–0.03) in dichloromethane. [e] nd: not detect.

(a) (b)

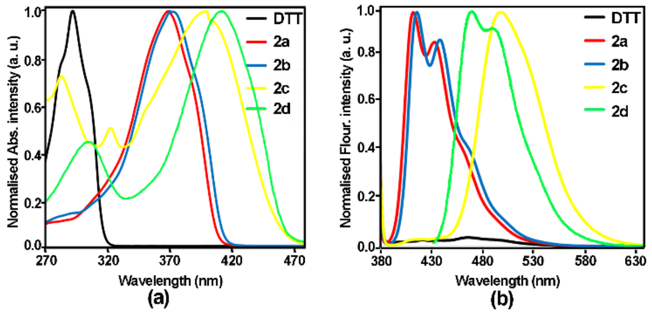

Figure 2. (a) Normalized UV-vis absorption and (b) fluorescence emission spectra of compounds **2** recorded in dichloromethane solutions at ~ $10^{-5} – 10^{-7}$ M at 25 °C.

Figure 3 shows the effect of concentration on the fluorescence emission of compound **2b** in dichloromethane at room temperature. On increasing the concentration of **2b** from 1.0 × 10^{-8} M (line 1) to 1.0 × 10^{-4} M (line 10), the fluorescent intensity of this emission band gradually increased. This result strongly indicated that this compound does exhibit excimer at a concentration of 10^{-5} M and even higher concentrations. This evidence also indicated that the attachment of **2b** from getting close enough to result in excimer emission at high concentrations. The reason is the fact that the attachment of sterically hindered substituents at the 2,6-positions in DTT can directly inhibit the close face-to-face π-stacking interactions between neighbouring DTT units. Similarly, the results based on monomer **2c** also provide further evidence of this (Figure S9).

Furthermore, the effect on the photo-physical properties of monomers **2b**, **2c** have been examined in solvents of various polarity, such as cyclohexane (a), tetrahydrofuran

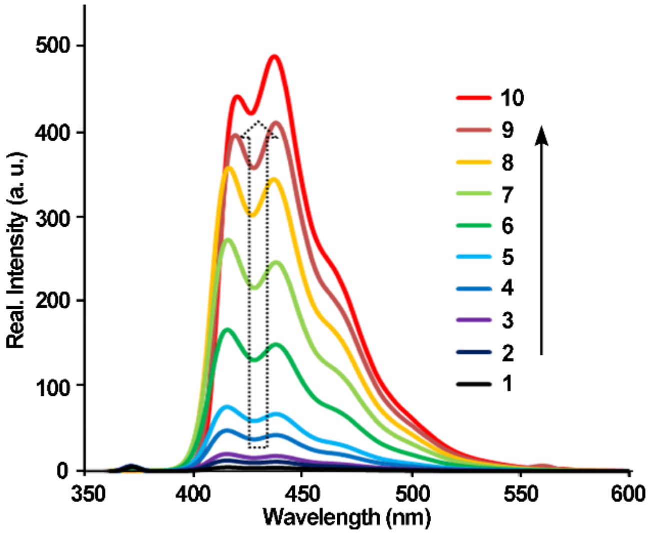

Figure 3. Effect of concentration on the fluorescence emission spectra of **2b** recorded in CH_2Cl_2 at 25 °C. (1) 1.0 × 10^{-8} M, (2) 2.5 × 10^{-8} M, (3) 1.0 × 10^{-7} M, (4) 2.5 × 10^{-7} M, (5) 1.0 × 10^{-6}, (6) 2.5 × 10^{-6} M, (7) 5.0 × 10^{-6} M, (8) 2.5 × 10^{-5} M, (9) 5.0 × 10^{-5} M, (10) 1.0 × 10^{-4} M.

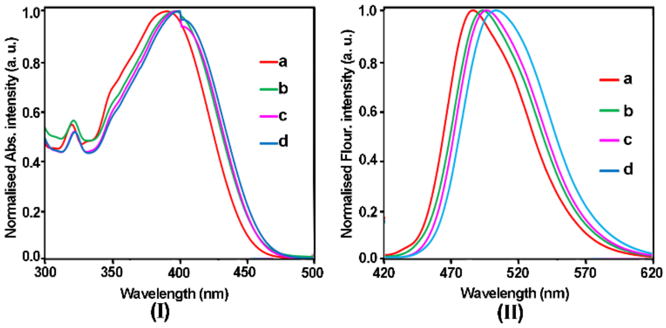

Figure 4. Normalised UV-Vis absorption spectra of **2c** (I), and fluorescence spectra of **2c** (II) recorded in (a) cyclohexane, (b) THF, (c) CH_2Cl_2, (d) DMF at ca. 10^{-5} M – 10^{-7} M at 25 °C.

(b), dichloromethane (c), and *N,N*-dimethylformamide (d). The solvent dependence of the absorption and fluorescence spectra of **2b**, **2c** are displayed in Figure 4 and in the supporting information (Figure S10), and the optical data are summarized in Table S1. Each monomer shows slight solvatochromism in the absorption spectra and emission spectra. For instance, for compound **2c**, a change of solvent from nonpolar cyclohexane to polar DMF caused only a very slight positive bathochromic shift in the π–π^* absorption band from 390 to 399 nm (Figure 4a). On the other hand, in the case of the emission spectra of **2c**, we observed substantial positive bathochromism with a peak seen at around 487 nm in cyclohexane (Figure 4b), while we observed a broad and red-shifted emission with only one peak at $\lambda_{\mathrm{em\ max}}$ = 504 nm in the high polarity solvent DMF. Similar results were also observed in the absorption spectra and emission spectra for **2b** (Figure S10). These results indicated that μ_e (dipole moment of **2** in the excited state) should be larger than μ_g (the dipole moment of **2** in the ground state).[18]

To provide explicit evidence for the energy states, in particular, the effect of the introduction of different donor moieties on the π-extended DTT, the energy bandgaps of D-π-D compounds were further evaluated by density functional theory (DFT) calculations at the B3LYP/6-31G* level. As shown in Figure 5, the HOMOs and LUMOs of the compounds **2a**–**2c** are almost distributed over the entire molecular skeleton. However, it is noteworthy that the HOMO-LUMO energy gaps of the compounds **2** are lower than the parent compound DTT due to the effect of the substituents on the energies of the molecular orbitals. Moreover, the optical properties combined with the DFT results indicated that the pyrene group may be playing a dominant role. On the other hand, the HOMOs of **2d** are mainly distributed over the entire molecule, while the LUMOs are mostly localized on the rigid DTT core. The closely separated HOMOs and LUMOs resulted from the presence of the strong electron-donating nature of the *N*,*N*-diphenylaminophenyl groups. In this process, the ICT plays an important role in lowering the energy gap (ΔE),[19] which is consistent with the excitation spectra.

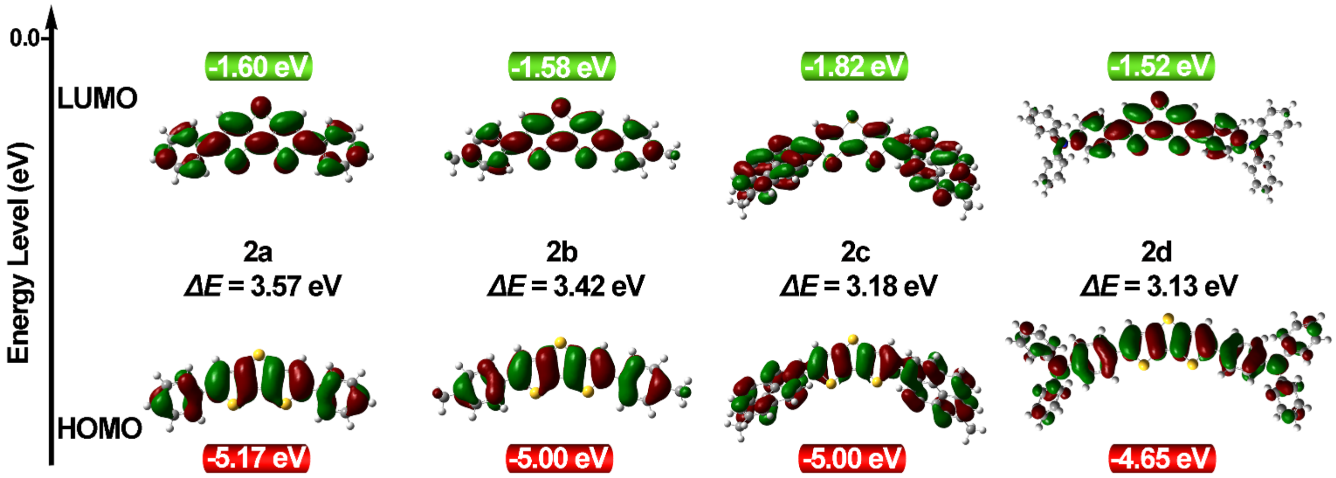

Figure 5. HOMO/LUMO energy levels and frontier molecular orbitals obtained from DFT calculations on the DTT and compounds **2** with optimized geometries. ΔE is an energy bandgap of the DTT and compounds **2** estimated from difference between the HOMO and LUMO values.

Conclusions

In summary, four stable D-π-D monomers were synthesized by a modified Suzuki-Miyaura cross-coupling reaction in reasonable yield. The extended π-conjugated structures were fully characterised by X-ray crystallography, NMR spectroscopy, optical properties, and DFT calculations. In comparison to the DTT core, all of the D–π–D type molecules possess higher fluorescence efficiency in the solid state than in dilute solution. The emission spectra of **2** exhibited an observable red shift. The introduction of different types of electron-donating substituents is not only useful in the design of novel chromophores based on DTT and other organic molecules but could also enable the preparation of high-efficiency opto-electronic materials for use in organic semiconductor, as well as in solar cells.

Experimental

All melting points are uncorrected. The ^{1}H NMR spectra were recorded at 300 MHz on a Nippon Denshi JEOL FT-300 NMR spectrometer in deuteriochloroform with TMS as an internal reference. The IR spectra were obtained as KBr pellets with a Nippon Denshi JIR-AQ2OM spectrometer. UV/Vis spectra were obtained with a Perkin–Elmer Lambda 19 UV/Vis/NIR spectrometer in various organic solvents. Fluorescence spectroscopic studies were performed in various organic solvents in a semimicro fluorescence cell (Hellma®, 104F-QS, 10 × 4 mm, 1400 µL) with a Varian Cary Eclipse spectrophotometer. Fluorescence quantum yields were measured using absolute methods. Mass spectra were obtained with a Nippon Denshi JMS-HX110A Ultra-high Performance Mass Spectrometer at 75 eV using a direct-inlet system. Elemental analyses were performed with a Yanaco MT-5 analyser.

General Procedure for the Suzuki – Miyaura Coupling Reaction Towards the Synthesis of 2a–d: 2,6-Dibromodithieno[3,2-*b*:2',3'-*d*]thiophene **1** (0.56 mmol), Pd(PPh$_3$)$_4$ (2.3 mol%), Na$_2$CO$_3$ (2 M) and a arylboronic acid (1.5 mmol) were added to a degassed solution of dry THF (10 mL) under argon. The resulting mixture was heated to reflux for the time mentioned in the individual cases. The reaction mixture was then cooled to room temp., quenched with saturated solution of ammonium chloride, and extracted with CHCl$_3$. The solvent was removed to give the crude reaction mixture, which was further worked up as indicated in the individual cases.

Synthesis of 2,6-bis(4-phenyl)dithieno[3,2-*b*:2',3'-*d*] thiophene (2a)

Pd(PPh$_3$)$_4$ (15 mg, 2.3 mol%) and aqueous Na$_2$CO$_3$ (7.55 mL; 2 M) solution were added to a solution of 2,6-dibromodithieno[3,2-*b*:2,3-*d*]thiophene (200 mg, 0.56 mmol) and phenylboronic acid (184 mg, 1.5 mmol) in dry THF (11 mL). The mixture was heated to reflux for 24 h and then poured into a saturated solution of ammonium chloride and extracted with CHCl$_3$ three times. Then, the combined organic phase was washed with brine, dried over MgSO$_4$, and evaporated to dryness. The crude product was purified by silica gel, using petroleum ether as the eluent, to give a yellow solid **2a** in a yield of 74.3 % (145 mg); m.p: 277–280 ℃. ^{1}H-NMR (300 MHz, CDCl$_3$): δ_H (ppm) 7.27 (s, 2H), 7.37 (d, *J* =8.43Hz, 4H), 7.45 (s, 2H), 7.56 (d, *J* =8.43Hz, 4H). ^{13}C-NMR[14]. MS: m/z: 348.01 (M$^+$). Elemental Analysis. $C_{20}H_{12}S_3$ (348.50): calc. C. 68.93, H. 3.47, Found: C. 68.71, H. 3.36.

Synthesis of 2,6-bis(4-*tert*-butylphenyl)dithieno[3,2-*b*:2',3'-*d*]thiophene (2b)

Pd(PPh$_3$)$_4$ (15 mg, 2.3 mol%) and aqueous Na$_2$CO$_3$ (7.55 mL; 2 M) solution were added to a solution of 2,6-dibromodithieno[3,2-*b*:2,3-*d*]thiophene (200 mg, 0.56 mmol) and 4-*tert*-butylphenylboronic acid (248 mg, 1.39 mmol) in dry THF (11 mL). The mixture was heated to reflux for 24 h and then poured into a saturated solution of ammonium chloride and extracted with CHCl$_3$ three times. Then, the combined organic phase was washed with brine, dried over MgSO$_4$, and evaporated to dryness. The filtrate was condensed and purified on column chromatography with hexane as CHCl$_3$ (9: 1). The residue was recrystallized from hexane gave 70 mg (27 %) of compound **2b** as yellow needle crystals; m.p: 290 ℃. ^{1}H-NMR (300 MHz, CDCl$_3$): δ_H (ppm) 1.36 (s, 18H), 7.44 (d, *J* = 8.43Hz, 4H), 7.48 (s, 2H), 7.59 (d, *J* = 8.43Hz, 4H). ^{13}C-NMR (400 MHz, CDCl$_3$): δ_C (ppm) 151.1, 145, 141.5, 131.8, 126, 125.4, 116.1, 34.7, 31.3. MS: m/z: 460.08 (M$^+$). Elemental Analysis. $C_{28}H_{28}S_3$ (460.71): calc. C. 72.99, H. 6.13, Found: C. 72.71, H. 6.16.

Synthesis of 2,6-bis(7-*tert*-butyl-1-pyrenyl)dithieno[3,2-*b*:2',3'-*d*]thiophene (2c)

Pd(PPh$_3$)$_4$ (15 mg, 2.3 mol%) and aqueous Na$_2$CO$_3$ (7.55 mL; 2 M) solution were added to a solution of 2,6-dibromodithieno[3,2-b:2,3-d]thiophene (200 mg, 0.56 mmol) and 7-*tert*-butyl-1-(4,4,5,5-tetramethyl-1,3,2-dioxaborolane-2yl)pyrene (542 mg, 1.5 mmol) in dry THF (11 mL). The mixture was heated to reflux for 24 h and then poured into a saturated solution of ammonium chloride and extracted with CHCl$_3$ three times. Then, the combined organic phase was washed with brine, dried over MgSO$_4$, and evaporated to dryness. The filtrate was condensed and purified on column chromatography with hexane. The residue was recrystallized from hexane gave 60 mg (29 %) of **2c** as a yellow powder; m.p: 332 ℃. ^{1}H-NMR (300 MHz, CDCl$_3$): δ_H (ppm) 1.361 (s, 18H), 7.64 (s, 2H), 8.07–8.23 (m, 14H), 8.62 (d, *J* = 9.0Hz, 2H). ^{13}C-NMR (300 MHz, CDCl$_3$): δ_C (ppm) 149.5, 143.4, 141.1, 131.3, 130.8, 129.3, 128.9, 128.5, 128.2, 128.1, 127.2, 125.0, 124.6, 124.4, 122.9, 122.8, 122.5, 121.3, 35.3, 31.9, 29.7 MS: m/z: 708.12 (M$^+$). Elemental Analysis. $C_{49}H_{40}S_3$ (708.99): calc. C. 81.31, H. 5.12, Found: C. 81.36, H. 5.14.

Synthesis of 2,6-bis((4-*N*,N-diphenylamono)phenyl)- dithieno[3,2-*b*:2',3'-*d*]thiophene (2d)

Pd(PPh$_3$)$_4$ (15 mg, 2.3 mol%) and an aqueous Na$_2$CO$_3$ (7.55 mL; 2 M) solution were added to a solution of 2,6-dibromodithieno[3,2-*b*:2,3-*d*]thiophene (200 mg, 0.56 mmol) and 4-*N*,*N*-diphenylaminophenyl boronic acid (401 mg, 1.39 mmol) in dry THF (11 mL). The mixture was heated to reflux for 24 h and then poured into a saturated solution of ammonium chloride and extracted with CHCl$_3$ three times. Then, the combined organic phase was washed with brine, dried over MgSO$_4$, and evaporated to dryness. The filtrate was condensed and purified on column chromatography with hexane and CHCl$_3$ (9: 1). The residue was recrystallized from hexane to give 176 mg (46 %) of a mixture of compound **2d** as a brown solid; m.p: 302℃. ^{1}H-NMR (400 MHz, CDCl$_3$): δ_H (ppm) 7.07 (m, 5H), 7.14 (d, J =8.3Hz, 4H), 7.29 (d, J =7.3Hz, 4H), 7.40 (s, 1H), 7.49 (d, J =8.3Hz, 2H). ^{13}C-NMR (400 MHz, CDCl$_3$): δ_C (ppm) 147.8, 147.6, 144.9, 141.8, 129.6, 127.6, 126.7, 125.7, 124.9, 123.7, 116.7, 115.7. MS: m/z: 682.13 (M$^+$). Elemental Analysis. C$_{28}$H$_{28}$S$_3$ (682.92): calc. C. 77.38, H. 4.43, Found: C. 77.36, H. 4.44.

Single-crystal X-ray diffraction measurements

A suitable single crystal (*ca.* 0.25 × 0.20 × 0.10 mm^3) was taken up and mounted on a Bruker APEX 2 CCD diffractometer equipped with fine-focus sealed tube radiation source for **2b**.[20] Detailed crystallographic data for **2b**: C$_{28}$H$_{28}$S$_3$, M = 460.71, orthorhombic, *Pna*2$_1$, a = 37.342 (6), b = 10.561 (18), c = 5.9981 (10) Å, α = 90.00, β = 90.00, γ = 90.00, V = 2365.5 (7) Å^3, Z = 4, D_{calc} = 1.294 g/cm^3, T = 113 K; 30309 reflections measured on a Rigaku Saturn CCD diffractometer, of which 4288 were independent, data corrected for absorption on the basis of symmetry equivalent and repeated data (min and max transmission factors: 0.455 and 0.745) and Lp effects, R_{int} = 0.0447, structure solved by direct methods (Sir2002), F^2 refinement, R_1 = 0.0302 for 286 data with $F^2 > 2\sigma(F^2)$, wR_2 = 0.0751 for all data, 286 parameters, Crystallographic data (excluding structure factors) for the structures in this paper have been deposited with the Cambridge Crystallographic Data Centre as supplementary publication numbers CCDC 1520658. Copies of the data can be obtained, free of charge, on application to CCDC, 12 Union Road, Cambridge CB2 1EZ, UK [fax: 144-1223-336033 or e-mail: deposit@ccdc.cam.ac.uk].

Acknowledgements

This work was performed under the Cooperative Research Program of "Network Joint Research Center for Materials and Devices (Institute for Materials Chemistry and Engineering, Kyushu University)". We would like to thank the National Science Foundation of China (No: 21602014), the Scientific Research Foundation for the Returned Overseas Chinese Scholars, and the State Education Ministry, The Scientific Research Common Program of Beijing Municipal Commission of Education, the OTEC at Saga University and the International Cooperation Projects of Guizhou Province (No. 20137002), The EPSRC is thanked for an overseas travel grant to C.R.

Notes and references

[a] *Department of Applied Chemistry, Faculty of Science and Engineering, Saga University, Honjo-machi 1, Saga 840-8502 Japan, E-mail: yamatot@cc.saga-u.ac.jp.*
[b] *School of Printing and Packaging Engineering, Beijing Institute of Graphic Communication, 1 Xinghua Avenue (Band Two), Daxing, Beijing, 102600, P. R. China*
[c] *Institute for Materials Chemistry and Engineering, Kyushu University, 6-1, Kasugakoen, Kasuga 816-8580, Japan*
[d] *School of Mathematics and Physical Sciences, The University of Hull, Cottingham Road, Hull, Yorkshire, HU6 7RX, UK*

† Electronic Supplementary Information (ESI) available: Details of single-crystal X-ray crystallographic data. ^{1}H, ^{13}C NMR of **2**. For ESI and other electronic format see DOI: 10.1039/x0xx00000x

‡ Footnotes relating to the main text should appear here. These might include comments relevant to but not central to the matter under discussion, limited experimental and spectral data, and crystallographic data.

1 (*a*) G. R. Hutchison, M. A. Ratner and T. J. Marks, *J. Am. Chem. Soc.*, 2005, **127**, 16866–16881; (*b*) S. J. Su, C. Cai and J. Kido, *Chem. Mater.*, 2011, **23**, 274–284; (*c*) H. Usta, A. Facchetti and T. J. Marks, *Acc. Chem. Res.*, 2011, **44**, 501– 510; (*d*) D. J. Schipper, L. C. H. Moh, P. Müller and T. M. Swager, *Angew. Chem., Int. Ed.*, 2014, **53**, 5847–5851; (*e*) A. J. Eberhart, H. Shrives, Y. T. Zhang, A. Carrer, A. V. S. Parry, D. J. Tate, M. L. Turner and D. J. Procter, *Chem. Sci.*, 2016, **7**, 1281–1285; (*f*) Y. Levratovsky and E. Gross, *Faraday Discuss.*, 2016, **188**, 345–353.

2 (*a*) J. N. Wilson and E. T. Kool, *Org. Biomol. Chem.*, 2006, **4**, 4265–4274; (*b*) T. Knaus, F. G. Mutti, L. D. Humphreys, N. J. Turner and N. S. Scrutton, *Org. Biomol. Chem.*, 2015, **13**, 223–233.

3 H. Zollinger, *Color Chemistry*, 3rd ed., Wiley-VCH, New York, 2001.

4 (*a*) D. Best and H. W. Lam, *J. Org. Chem.*, 2014, **79**, 831–845; (*b*) J. Liu, C. Q. Wang, C. L. Xu, L. M. Song and R. S. Na, *Nongyao*, 2014, **53**, 625–630.

5 T. Eicher and S. Hauptmann, *The Chemistry of Heterocycles*, Wiley-VCH Verlag: Weinheim, 2003; Chapter 5, p 52.

6 (*a*) J. Roncali, *Chem. Rev.*, 1992, **92**, 711–738; (*b*) J. Roncali, *Chem. Rev.*, 1997, **97**, 173–205.

7 (*a*) T. Yamamoto, T. Nishimura, T. Mori, E. Miyazaki, I. Osaka, K. Takimiya, *Org. Lett.*, 2012, **14**, 4914–4917; (*b*) J. W. Shi, L. Xu, Y. B. Li, M. Jia, Y. H. Kan, H. Wang, *Org. Electron*, 2013, **14**, 934–941.

8 (*a*) M. Mazzeo, V. Vitale, F. D. Sala, M. Anni, G. Barbarella, L. Fabaretto, G. Sotgiu, R. Cingolani, G. Gigli, *Adv. Mater.*, 2005, **17**, 34–39; (*b*) Y. Shibano, T. Umeyama, Y. Matano, H. Imahori, *Org. Lett.*, 2007, **10**, 1971–1974; (*c*) L. Zhang, L. Tan, Z. Wang, W. Hu, D. Zhu, *Chem. Mater.*, 2009, **21**, 1993–1999.

9 (*a*) J. D. Huang, S. H. Wen, K. L. Han, *Chem.-Asian J.*, 2012, **7**, 1032–1040; (*b*) M. E. Cinar, T. Ozturk, *Chem. Rev.*, 2015, **115**, 3036–3140.

10 (*a*) L. Li, C. M. Zhao, H. Wang, *Chem. Rec.*, 2016, **16**, 797–809; (*b*) X. Feng, J. Y. Hu, C. Redshaw, T. Yamato, *Chem. Eur. J.*, 2016, **22**, 11898-11916.

11 (*a*) T. Oyamada, S. Akiyama, M. Yahiro, M. Saigou, M. Shiro, H. Sasabe, C. Adachi, *Chem. Phys. Lett.*, 2006, **421**, 295–299; (*b*) H. Shimizu, K. Fujimoto, M. Furusho, H. Maeda, Y. Nanai, K. Mizuno, M. Inouye, *J. Org. Chem.*, 2007, **72**, 1530–1533; (*c*) M. Uchimura, Y. Watanabe, F. Araoka, J. Watanabe, H. Takezoe, G. Konishi, *Adv. Mater.*, 2010, 22, 4473–4478.

12 M. Q. He, F. X. Zhang, *J. Org. Chem.*, 2007, **72**, 442–451.

13 G. A. Sotzing, J. R. Reynolds, P. J. Steel, *Chem. Mater.*, 1996, **8**, 882–889.

14 Y. M. Sun, Y. Q. Liu, Y. Y. Lin, Z. Y. Wang, C. A. Di, K. Xiao, X. M. Chen, W. F. Qiu, B. Zhang, G. Yu, W. P. Hu and D. B. Zhu, *Adv. Funct. Mater.*, 2006, **16**, 426–432;

15 A. Facchetti, M. H. Yoon, C. L. Stern, G. R. Hutchison, M. A. Ratner, T. J. Marks, *J. Am. Chem. Soc.*, 2004, **126**, 13480–13501.

16 (*a*) R. Lartia, C. Allain, G. Bordeau, F. Schmidt, C. Fiorini-Debuisschert, F. Charra, M. P. Teulade-Fichou, *J. Org. Chem.*, 2008, **73**, 1732–1744; (*b*) C. L.Droumaguet, A. Sourdon, E. Genin, O. Mongin, M. Blanchard-Desce, *Chem. Asian J.*, 2013, **8**, 2984–3001; (*c*) S. Karmakar, D. Maity, S. Mardanya, S. Baitalik, *J. Phys Chem. A*, 2014, **118**, 9397–9410; (*d*) X. Chen, X. Sang, Q. Zhang, *RSC Adv.*, 2015, **5**, 53211–53219.

17 (*a*) A. K. Pati, S. J. Gharpure and A. K. Mishra, *Faraday Discuss.*, 2015, **177**, 213–235; (*b*) V. K. Gupta and R. A. Singh, *Faraday Discuss.*, 2016, 10.1039/c6fd00158k.

18 (*a*) Mataga, N.; Kaifu, Y.; Koizumi, M. *Bull. Chem. Soc. Jpn.* **1956**, *29*, 465–470; (*b*) Lippert, E. *Z. Elektrochem* **1957**, *61*, 962–975.

19 C. Z. Wang, J. H. Do, T. Akther, X. Feng, L. Horsburgh, M. R. J. Elsegood, C. Redshaw and T. Yamato, *Tetrahedron*, 2016, *Online*, 10.1016/j.tet.2016.11.077.

20 APEX 2 & SAINT 2012, software for CCD diffractometers. Bruker AXS Inc. Madison, USA.